Iterative color-multiplexed, electro-optical processor

Demetri Psaltis, David Casasent, and Mark Carlotto

Carnegie-Mellon University, Department of Electrical Engineering, Pittsburgh, Pennsylvania 15213

A noncoherent optical vector–matrix multiplier using a linear LED source array and a linear P-I-N photodiode detector array has been combined with a 1-D adder in a feedback loop. The resultant iterative optical processor and its use in solving simultaneous linear equations are described. Operation on complex data is provided by a novel color-multiplexing system.

I. Introduction

In an effort to increase the flexibility of optical systems and to design optical processors that are more easily fabricated, Cutrona[1] suggested a simple vector–matrix multiplier in 1965. This system was capable of performing any linear transformation and was thus not limited to space-invariant operations. Since then, many similar optical systems have been reported, including extensive architecture studies,[2] feedback systems,[3] systems using multiple[4] and single[5] LED sources, matrix–matrix multipliers,[4] and discrete-Fourier-transform systems[6].

In this Letter we combine much of this previous work utilizing recent advances in LED's and detectors into an iterative optical processor. The novel aspects of this work are the iterative feedback concept and its application to solving matrix equations (Section II) and a new color-multiplexing method that enables the system to handle complex data vectors and matrices (Section III). A discussion of several applications of this system and initial experimental results are included in Section IV.

II. Iterative Optical Processor

The iterative optical processor that we have assembled is shown schematically in Fig. 1. The P_1–P_2–P_3 portion of the system is similar to one described earlier.[6] A linear N-element LED input array at P_1 is spatially modulated by the components A_n of the input vector **A**. Plane P_1 is imaged vertically onto P_2. The light from each LED is spread horizontally across the corresponding row at P_2. Stored at P_2 is the $N \times M$ matrix B, where b_{nm} is the transmittance of element (n,m). The mask at P_2 is then focused vertically and imaged horizontally onto a linear detector array at P_3. The output from the detector (m) is thus

$$C_m = \sum_n A_n b_{nm}, \qquad (1)$$

which is the scalar form of the vector–matrix product

$$C = BA. \qquad (2)$$

The much more formidable problem is to determine **A** given B and **C**, i.e., to solve

$$A = B^{-1} C. \qquad (3)$$

Using the iterative algorithm

$$A_{i+1} = (I - B)A_i + C, \qquad (4)$$

we can find **A** when the i and $i + 1$ estimates A_i and A_{i+1} are equal, i.e., when the iterative equation in Eq. (4) converges. In this case Eq. (4) reduces to $C = BA$, and hence **A** is given by Eq. (3). To realize Eq. (4) in the system of Fig. 1, we input an initial estimate A_i of **A** into P_1, and as the P_2 mask we use $(I–B)$, where I is the identity matrix. At P_3 we obtain $(I–B)A_i$, and at the output of the parallel adder we find A_{i+1} given by Eq. (4). This value is then reinserted into the LED's at P_1. On the next iteration we obtain A_{i+2} at the output of the adder. These iterations continue until $A_i = A_{i+1}$. At this point, we have the solution **A** to Eq. (3).

III. Color Multiplexing

To accommodate complex data vectors and matrices, we can decompose each complex input vector component A_n into its projections on the $0°$, $120°$, and $240°$ axes (represented by $\hat{0}$, $\hat{1}$, and $\hat{2}$, respectively) in the complex plane.[7,8] Representing each b_{nm} similarly, we can rewrite Eq. (2) as

$$
\begin{aligned}
C_{\hat{0}} + C_{\hat{1}} + C_{\hat{2}} &= (B_{\hat{0}} + B_{\hat{1}} + B_{\hat{2}})\,(A_{\hat{0}} + A_{\hat{1}} + A_{\hat{2}}) \\
&= (B_{\hat{0}}A_{\hat{0}} + B_{\hat{1}}A_{\hat{2}} + B_{\hat{2}}A_{\hat{1}})_{\hat{0}} \\
&\quad + (B_{\hat{1}}A_{\hat{0}} + B_{\hat{2}}A_{\hat{2}} + B_{\hat{0}}A_{\hat{1}})_{\hat{1}} \\
&\quad + (B_{\hat{2}}A_{\hat{0}} + B_{\hat{0}}A_{2} + B_{\hat{1}}A_{\hat{1}})_{\hat{2}}. \qquad (5)
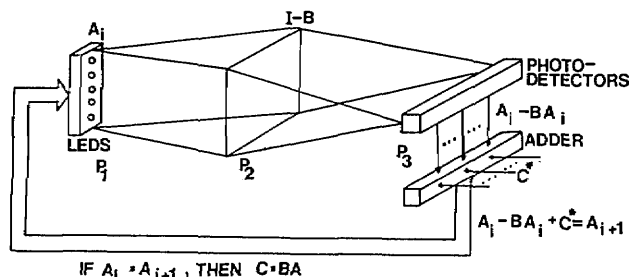\end{aligned}
$$

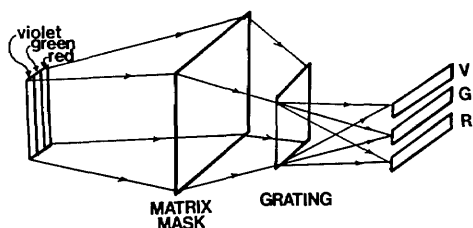Fig. 1. Schematic diagram of an iterative optical processor.

Fig. 2.   Schematic diagram of a color-multiplexed optical processor.

From Eq. (5), we see that by properly arranging the location of the components of B and by properly combining the various outputs at P_3, complex vector–matrix multiplication is possible.

This technique increases the size of the LED array required at P_1 by a factor of 3 and the space–bandwidth product (SBWP) of the P_2 mask by a factor of 9. To avoid this, color multiplexing can be utilized. The schematic diagram of such a system is shown in Fig. 2. Three input LED arrays with nonoverlapping spectra are modulated in parallel at P_1 with the three complex components $A_{\hat{0}}$, $A_{\hat{1}}$, and $A_{\hat{2}}$ of A. All three linear LED arrays simultaneously illuminate the mask B at P_2 as before. To separate the three components $C_{\hat{0}}$, $C_{\hat{1}}$, and $C_{\hat{2}}$ of C at P_3, a grating is inserted between P_2 and P_3. This separates the three colors vertically at P_3, where the three components of C are separately detected on three linear photodiode arrays. Summation of the proper photodiode outputs at P_3 yields the correct complex vector–matrix product. An iterative version of this color-multiplexed system follows directly from Fig. 2. The advantages of such a system are obviously a reduction by three in the 1-D SBWP of the input P_1 array and a reduction by three in the SBWP of the P_2 mask (only horizontal spatial multiplexing in the mask elements is needed). The nonuniqueness of the complex number representation in Eq. (5) can be avoided by subtracting the smallest component from the rest.

IV.   Experimental Confirmation

The inherent parallelism afforded by the system's architecture allows us to increase N and hence the SBWP without affecting the system's speed (or vice versa). Corrections for static and dynamic LED source errors as well as P_2 mask errors are also directly included in such an iterative feedback system. The system that we are currently fabricating uses $N = 20$ input LED's (present LED and laser-diode technology can easily extend this to $N = 100$). To reduce support electronics, input and output multiplexing is used. To reduce the effects of nonlinear LED source response and to increase system accuracy, pulse-width modulation of both the LED output and the P_2 mask is employed. This increases the cycle time of the system to 1 μsec. Although 10-nsec cycle times are possible with amplitude modulation and without electronic multiplexing, 1-μsec cycle times and the 8-bit accuracy that we expect to obtain are still admirable performance characteristics.

The absolute maximum size of the input LED array

is ultimately determined by the diffraction limit of the optics used in the system. To avoid this limitation on our system, we are considering several designs that will eliminate the need for optical elements (lenses). One such approach is the use of fiber-optic bundles that would transfer the light from the LED's to the mask and from the mask to the detector array. A second approach involves integrating the source, mask, and detector in a single device by the use of long rectangular source and detector elements.

The original proposed use for this system was as an adaptive phased-array radar signal processor.[9] To demonstrate the use of this iterative processor for this application, we considered the simple scenario of a single noise source and a two-element receiver array with receiver noise also present. For this application, the optimum weight vector A to be applied to the array is related to the covariance matrix B of the noise field and the steering vector C by

$$C^* = BA. \tag{6}$$

To solve Eq. (6) using the system of Fig. 1, we computed B for the case under study and fabricated a 6 × 6 element pulse-width modulated mask $(I–B)$ at P_2. A prototype system with 8 input LED's and a 20-element P-I-N detector array was used in these initial experiments. An initial estimate A_i for A was fed to 6 of the 8 input LED's. The vector–matrix product $(I–B)A_1$ was formed at P_3. After addition of C^*, we obtain the next iteration A_{i+1} for A. This process is continued until $A_i = A_{i+1}$. The P_3 outputs at selected iteration steps are shown in Fig. 3. As seen, the A outputs increase at each iteration closer to the final value. After seven iterations, all six A-component outputs are within 10% of their final values and within several per cent of
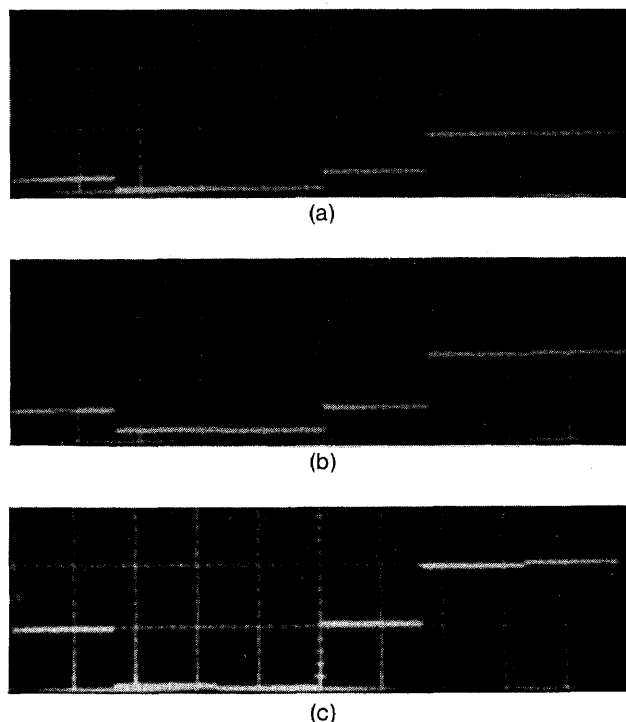

(a)

(b)

(c)

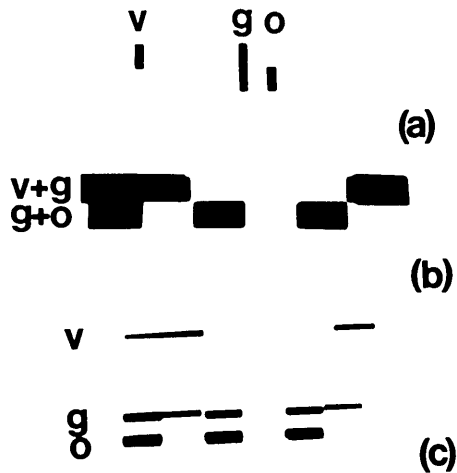Fig. 3.   Output-plane patterns at selected iterations.

Fig. 4. Color-multiplexed complex vector–matrix multiplication. (a) Input, (b) mask output, (c) system output. (Printed in black and white: v, violet; g, green; o, orange).

the theoretical values calculated by computer simulation.

The results of a color-multiplexed complex vector–matrix multiplication are shown in Fig. 4. For this experiment an arc-lamp source with three spectral lines (violet λ_1, green λ_2, and orange λ_3) was used as the source. A two-element input vector with components $\alpha_{\lambda_1} = (1,0)$, $\alpha_{\lambda_2} = (1,1)$, and $\alpha_{\lambda_3} = (0,1)$ was used as the 2 × 3 input [see Fig. 4(a)]. The output from a 2 × 6 mask B is shown in Fig. 4(b). Since λ_1 reads out row 1, λ_2 rows 1 and 2, and λ_3 row 3, turquoise- (violet plus green) and yellow- (green plus orange) colored light outputs result from P_2. The 3 rows (6 elements per row) in the P_3 output shown in Fig. 4(c) are violet (top row of P_2 mask), green (both rows), and orange (bottom row), and they represent the 3 × 6 = 18 possible cross products of Eq. (5). In practice, one detector array is used per row or color.

The iterative process is stable and will converge to the one correct solution for all initial choices of A_i if the magnitude of the eigenvalues of B are all less than 1 (this can be ensured by proper normalization of B). The feedback process can be stopped when A_i and A_{i+1} are sufficiently close.

V. Summary

Noncoherent optical-matrix multipliers have been found to be most useful when reconfigured as iterative systems to solve matrix equations. The use of color multiplexing allows complex vector–matrix multiplications to be realized and provides an added dimension to the optical processor. For example, use of color-multiplexing enables us to encode a 2-D pattern or many 1-D signals in the input plane for image or multichannel signal processing.

References

1. L. Cutrona, in *Optical and Electro-Optical Information Processing*, J. Tippett *et al.*, eds. (MIT Press, Cambridge, Massachusetts, 1965), pp. 97–98.
2. A. Edison and M. Nobel, Final Report, Contract AF19(628-4199), General Electric Company (November 1966).
3. D. Mengent *et al.*, U.S. Patent 3,525,856 (October 6, 1966).
4. W. Schneider and W. Fink, Opt. Acta **22**, 879 (1975).
5. M. Monahan, in *Digest of International Computing Conference, Washington, D.C.* (Institute of Electrical and Electronics Engineers, New York, 1975), pp. 25–33.
6. J. W. Goodman, A. R. Dias, and L. M. Woody, Opt. Lett. **2**, 1 (1978).
7. C. B. Burckhardt, Appl. Opt. **9**, 1949 (1970).
8. J. W. Goodman and L. M. Woody, Appl. Opt. **16**, 2611 (1977).
9. D. Psaltis, D. Casasent, and M. Carlotto, Proc. Soc. Photo-Opt. Instrum. Eng. **180** (to be published, 1979).